



Microscopic surface patterning by rubbing induced dewetting

Xueyun Zhang, Fengchao Xie, Ophelia K.C. Tsui*

Department of Physics and Institute of Nano Science and Technology, Hong Kong University of Science and Technology, Clear Water Bay, Hong Kong, China

Received 15 March 2005; received in revised form 18 June 2005; accepted 20 June 2005

Available online 20 July 2005

Abstract

We demonstrate a method to fabricate microscopic topographic patterns over a large area. The idea is based on anisotropic dewetting of a previously rubbed polymer film. Two types of patterns are demonstrated. One contains well aligned parallel micro-grooves with widths and separations of about 1 μm . The other contains striped domains of micro-grooves oriented parallel and orthogonal to the stripes in alternation. Although the pattern formation had been demonstrated on $2 \times 2 \text{ cm}^2$ substrates, this method is scalable to any substrate size and could offer an attractive low-cost alternative to photolithography and soft lithography in very large area applications.

© 2005 Elsevier Ltd. All rights reserved.

Keywords: Non-lithographic surface patterning; Thin film dewetting; Polymer thin films

1. Introduction

Fabrication of microelectronic circuits and digital storage media requires patterning surfaces in microscopic length scales. Among different patterning techniques, photolithography is the most developed and pervasive in microfabrication. Nevertheless, extensive efforts have been made in the recent decade to develop alternative methods to replace photolithography due to the expensive instrumentation and maintenance required of this technique. Beginning from the mid 1990s, a new class of lithographic methods known as soft lithography blossomed. In general, soft lithography involves the use of an elastomeric poly(dimethylsiloxane) (PDMS) stamp, possessing a topographic structure molded from a master, to replicate the structure of the master onto the target. Due to the different mechanisms involved in replicating the structure, a great variety of soft lithographic techniques were invented including micro-molding in capillaries [1], replica molding of a curable polymer [2] or a drying solution of resin [3], micro-transfer molding [4], solvent-assisted micro-contact molding [5], the ‘hot lift off’ method [6], and the lithographically controlled wetting method [7], etc.

More recently, the use of dewetting instability of polymer films for pattern formation has aroused much theoretical [8–10] and experimental interest [11–25]. The majority of ideas in this league are based on dewetting directed by a surface pattern inscribed on the supporting substrate [8–11,18] or a surface pattern inscribed on a stamp pressing against the dewetting film [19–23], or by an external field applied between the stamp and the film [24, 25]. A master or a stamp possessing the symmetry of the final pattern is needed in these methods. Huggins et al. proposed a new route to the production of anisotropic patterns, without the need for a master, by the rupturing of a spinodally unstable (i.e. spontaneously unstable) polymer film on a rubbed supporting surface [12]. Reasonably well defined periodicity from 3 to 9 μm was found in the patterns produced, controllable through the wavelength selectivity of the spinodal dewetting process [12]. Later it was found that dewetting of a previously rubbed polymer film could also produce anisotropic patterns including elongated Voronoi networks and parallel arrays of polymer beads [17]. Here, we show that by carefully controlling the conditions of dewetting for previously rubbed polymer films in the spinodal instability regime, patterns comprising highly extended parallel grooves about 1 μm wide can be produced. Combined with photolithography, patterns composed of striped domains of parallel grooves alternating between the longitudinal and transverse directions to the domain stripes are produced.

* Corresponding author. Tel.: +852 2358 7524; fax: +852 2358 1652.
E-mail address: phtsui@ust.hk (O.K.C. Tsui).

2. Experiment

The polymer used in this experiment is monodispersed polystyrene (PS) ($M_w = 13.7$ kg/mol, $M_w/M_n = 1.1$) purchased from Scientific Polymer Products (NY, USA). The glass transition temperature of the polymer was measured to be 90°C by differential scanning calorimetry (DSC). Polystyrene films of thickness about 6 nm were spin-coated onto cleaned silicon substrate covered with a thermal silicon oxide layer either 15 or 100 nm thick. All layer thicknesses were measured by means of variable angle spectroscopic ellipsometry (A. J. Woollam, Lincoln, NE, USA). Prior to use, we cleaned the substrates by first immersing them in a solution of H_2SO_4 and H_2O_2 mixture (in 10:1 volume ratio) at 120°C for 10 min. Thereafter, the substrates were thoroughly rinsed in deionized water and finally blow-dry by compressed nitrogen gas. The coated polymer films were pre-baked inside a vacuum oven at 100°C for 5 h to remove the residual solvent toluene. No sign of dewetting was detectable in the polymer film after pre-baking. Nano-groove defects were introduced to the hence pre-baked films by rubbing the films surface unidirectionally 20 times at a constant speed of 1 cm/s and a normal pressure of 5 g/cm^2 with a home-built apparatus [26].

Dewetting was performed in vacuum or in air above the glass transition temperature of the polymer. The resulting dewetted patterns were found to be the same in either annealing environment, but dewetting proceeds faster in air than in vacuum. Well ordered polymer lines were found obtainable through a careful control of the dewetting time (to be elaborated in the next section).

The dewetted morphology was transferred to the silicon dioxide underneath by the buffered oxide etchant (BOE) solution, a well-known wet etchant for silicon dioxide, by which the exposed regions of the silicon dioxide not covered by the polystyrene ridges in the dewetted pattern were etched away while the parts covered by the polystyrene were protected.

In making the second pattern containing striped domains of orthogonal grooves, fabrication of chromium stripes with $5\text{ }\mu\text{m}$ line-and-space by photolithography was involved. Chromium deposition was carried out with an Auto 306 Turbo e-beam evaporator by BOC Edwards Vacuum Technology (West Sussex, UK) equipped with a FTM6 film thickness monitor. Photolithography was performed in a contact aligner (AB-Manufacturing, Inc., San Jose, CA, USA) in a class 1000 clean room. Topographic morphology of the samples was characterized by a Seiko Instruments (Chiba, Japan) SPA-300HV atomic force microscope (AFM) operating in the non-contact mode. Optical images of the samples were obtained by an Olympus (NY, USA) BX60 polarizing microscope.

2.1. Fabrication of parallel groove pattern

Fig. 1 schematically shows the procedure we undertook

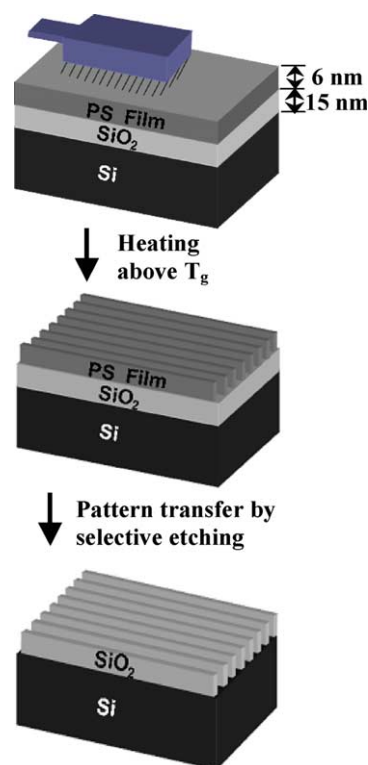


Fig. 1. Schematic illustration of the procedure to fabricate a parallel micro-groove pattern on a silicon substrate with a thermal oxide capping layer.

in producing the parallel groove pattern. The surface of the pre-baked polymer film was uni-directionally rubbed in a home-built apparatus (Fig. 1(a)). Then, the film was heated above the glass transition temperature to enable dewetting of the film until well ordered polymer lines parallel to the rubbing direction were formed (Fig. 1(b)) whereupon the film was quenched to room temperature. The dewetted pattern was transferred to the underlying silicon oxide by selective etching in a BOE solution. Upon removing the PS residue on the sample with toluene, a well ordered parallel groove pattern resulted on the substrate surface (Fig. 1(c)).

2.2. Fabrication of stripes of alternating horizontal and vertical grooves

Fig. 2 schematically shows the fabrication procedure, we used in fabricating the striped pattern of alternating horizontal and vertical micro-grooves. A chromium layer of about 5 nm in thickness was first deposited onto a silicon substrate possessing a 100 nm thick thermal oxide capping layer (Fig. 2(a)). A grating structure of $5\text{ }\mu\text{m}$ line-and-space was fabricated in the chromium film by photolithography. Then a PS film was spin-coated on top (Fig. 2(b)). The condition of spin-coating was one that would give a 6 nm thick film if the coated surface were flat (100) silicon covered by a native oxide layer. The resulting PS film on the Cr grating was found to have a thickness of about 5 nm to 6 nm both on the protruding Cr stripes and in the indented

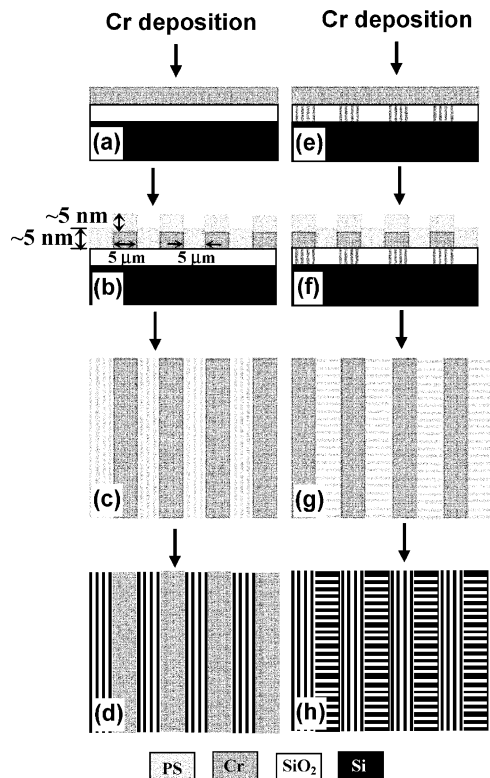


Fig. 2. Schematic illustration of the procedure to fabricate parallel stripes of alternating horizontal and vertical grooves.

regions. Accordingly, the coated PS conforms with the underlying grating structure very well as demonstrated by the AFM topographic images of the grating pattern just before and after spin-coating of the PS film on the grating in Fig. 3(a) and (b), respectively. The coated film was rubbed either parallel or perpendicular to the stripes. In the illustration shown in Fig. 2, rubbing parallel to the stripes assumes. Then the sample was heated above the glass transition temperature to obtain well order polymer lines (Fig. 2(c)). This polymer pattern was transferred to the silicon oxide layer beneath in the next step by BOE etching followed by rinsing in toluene to remove the polymer lines, which leaves 5 μm wide stripe domains of silicon oxide micro-grooves ($\sim 40 \text{ nm(H)} \times \sim 1 \mu\text{m(W)}$) on silicon equally spaced by 5 μm wide stripes of chromium (Fig. 2(d)). Upon removing the chromium stripes with phosphoric acid, on the resulting pattern was deposited a uniform layer of chromium with a thickness of about 5 nm (Fig. 2(e)). By means of photolithography and selective etching in phosphoric acid (that removes the exposed chromium), a grating structure of 5 μm line-and-space was fabricated in the chromium, so aligned that the silicon oxide micro-grooves were exactly covered by the chromium stripes. Then a PS film of $\sim 6 \text{ nm}$ thickness was deposited on top (Fig. 2(f)). This film was rubbed in a direction orthogonal to the silicon oxide micro-grooves already existed. Then, the sample was heated above the glass

transition temperature allowing the PS film to dewet into ordered polymer ridges (Fig. 2(g)). Finally, the polymer patterned was transferred into the underlying silicon oxide by BOE etching, following by sequential removal of the protective PS and chromium in toluene and phosphoric acid, respectively. These led to the final pattern with alternating stripes of horizontal and vertical micro-grooves (Fig. 2(h)).

3. Results and discussion

According to the result of Du et al. [17], thin film dewetting in PS/SiO₂/Si is dominated by the spinodal mechanism if the film thickness is below 13.3 nm, but becomes dominated by heterogeneous nucleation when the film thickness is above 13.3 nm. In here, the thickness of the PS films is 6 nm so the dewetting should be dominated by the spinodal mechanism. Fig. 4 displays the optical images of a 20-time-rubbed 6 nm thick dewetting PS film taken after the film was annealed at 115 °C in a vacuum oven for different cumulative times from 1 to 15 h. In comparing these images with those obtained from an unrubbed film with similar thickness (Fig. 6 of Ref. [17]), it is clear that rubbing engenders strong anisotropy in the dewetting morphology with the direction of anisotropy parallel to that of rubbing, consistent our previous finding [17].

By taking a closer look at the images shown in Fig. 4, one may immediately notice a key to the production of well aligned polymer lines, namely the heating time. As seen, if the heating time is too short, some of the polymer lines arising from spinodal amplification of the rubbing-induced nano-grooves may not be developed enough for pattern transfer (the valleys in the polymer line pattern need to be nearly touching the substrate surface in order for good pattern transfer to be possible). On the other hand, if the heating time is too long, the polymer lines grown from spinodal amplification of the nano-grooves may break up into short segments or droplets due to the Rayleigh instability [27]. From Fig. 4, a heating time of about 6 h is suitable for the annealing temperature used. Fig. 5(a) and (b) shows the AFM topographic images of the parallel groove pattern fabricated just before and after etching of the dewetted film in BOE, respectively. Fig. 5(c) shows the cross-sectional profiles of these structures along arbitrarily drawn lines shown in Fig. 5(a) and (b). Apart from the different heights (it is that of the polymer ridges before etching but is that of the silicon oxide $\sim 15 \text{ nm}$ after etching), the two profiles are very similar, which evidences the pattern transfer by BOE etching to be successful. From Fig. 5(c), the grooves are reasonably periodic with a periodicity of approximately 2 μm . Random sampling of the groove pattern revealed that the same structure prevails everywhere, confirming this technique to be applicable to large area applications. The inset of Fig. 5(a) and (b) display the two-dimensional Fourier transformation of the pattern shown in the respective main panel. Evidently, the patterns

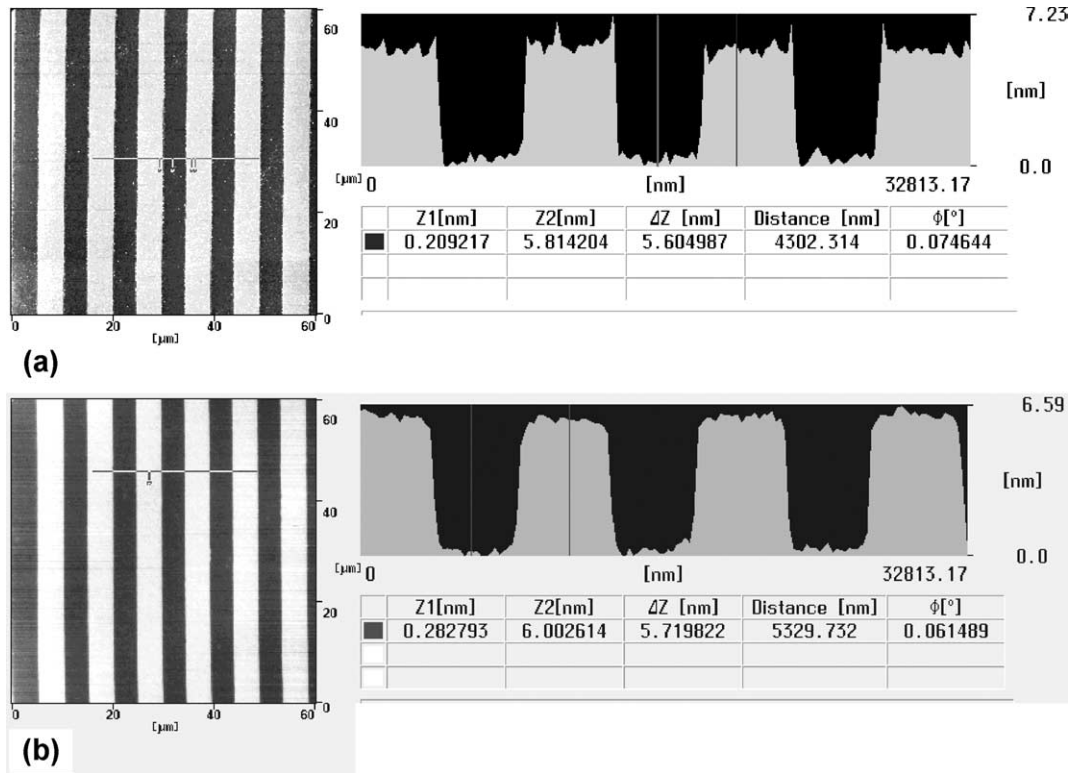


Fig. 3. AFM topographic images of the sample (a) just before and (b) just after spin-coating of the PS film on top of the Cr grating.

are composed of a distribution of periodicities about a modal wavelength, consistent with the Fourier spectrum expected from a spinodal process. According to the theory [17], the characteristic wavelength, λ_c , due to spinodal dewetting is given by $\lambda_c = (16\pi^3 \gamma A)^{1/2} h^2$ where γ is the surface tension of the polymer, A is the Hamaker constant of the polymer film and h is the film thickness. By substituting $\gamma = 31.4$ mN/m for PS [28] and $A = 1.8 \times 10^{-20}$ J for air/PS/SiO₂ [29] from the literature and $h = 6$ nm, we deduce that

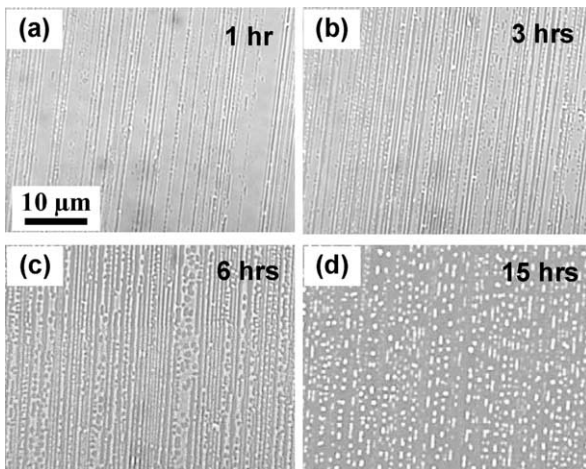
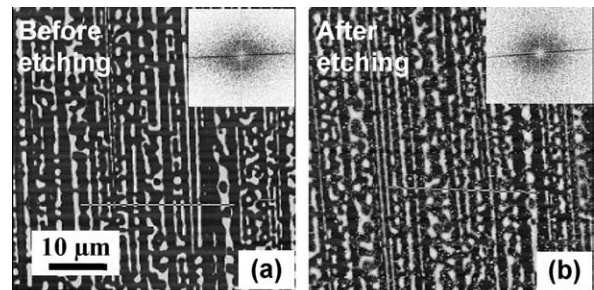


Fig. 4. Optical images of a dewetting 6 nm thick, 20-time-rubbed polystyrene film after annealing at 115 °C in vacuum oven for different cumulative times of (a) 1 h, (b) 3 h, (c) 6 h, and (d) 15 h. The scale bar is applicable to all images.

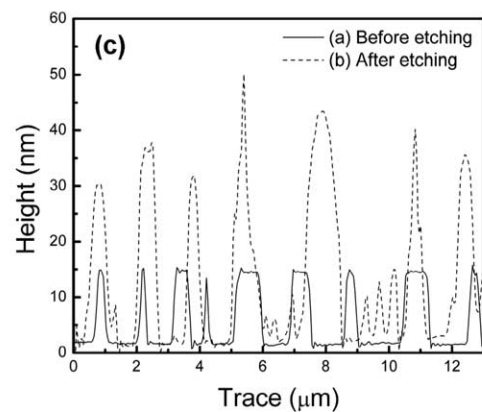


Fig. 5. AFM topographic images of the parallel micro-groove pattern (a) just before and (b) just after etching in BOE. The insets are the two-dimensional Fourier transformations of the real images shown in the main panel. (c) The cross-sectional profiles of the patterns displayed in (a) and (b) along arbitrarily drawn lines as shown. The scale bar in (a) applies to the image in (b).

the characteristic wavelength should be $1.1\ \mu\text{m}$, which is somewhat smaller than the period of $2\ \mu\text{m}$ noted from Fig. 5. Given that our patterns, with well developed ridges and valleys, must be well beyond the initial stage of dewetting, and that the characteristic length scale could easily double upon coarsening according to former experiment [30], the agreement is quite good indeed. On the basis that λ_c varies like h^2 , groove patterns with even smaller periods are achievable by the use of thinner films in dewetting.

Next, we discuss the data obtained in making the pattern with alternating horizontal and vertical micro-grooves. Fig. 6(a) and (b) displays the optical images of the sample after following the steps shown by Fig. 2(a)–(d) with the direction of rubbing (applied just before the state shown in Fig. 2(c)) being orthogonal and parallel, respectively, to the chromium stripes. Shown in Fig. 7 is the three-dimensional AFM topographic image of the final pattern we obtained in following the remaining steps in Fig. 2, demonstrating successful fabrication of the desired pattern.

Compared to the other existing lithographic methods, the structures produced by this method are not as regular. However, for applications exploiting only the anisotropy of the surface pattern, such as liquid crystal alignment [31,32] and some novel optical applications [33], the surface structures produced here are suitable. With the micro-grooves of being only $\sim 1\ \mu\text{m}$ wide (Figs. 6 and 7), similar structures may not be easily fabricated by the other lithographic methods, especially when the sample area exceeds $\sim 16\ \text{in}$. In such cases, either the resolution of the technique is insufficient as with typical industrial photolithography facilities, or the sample fabrication time is impractically too long as with serial processing methods like e-beam lithography, or the size of the stamp is not large enough as with soft lithography.

4. Conclusion

In conclusion, we have devised a simple, inexpensive method for the fabrication of large-area micro-groove patterns based on spinodal dewetting of polymer films. Two structures were demonstrated. One contains parallel grooves about $1\ \mu\text{m}$ wide, for which the fabrication process

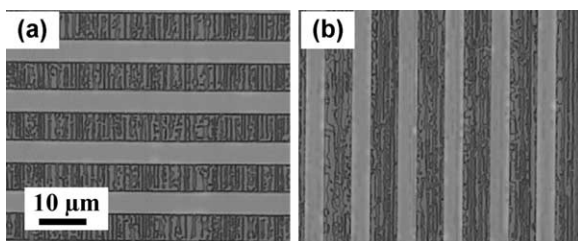


Fig. 6. Optical images of the samples obtained after following the steps illustrated by Fig. 2(a)–(d), with the rubbing direction (a) orthogonal and (b) parallel to the chromium stripes.

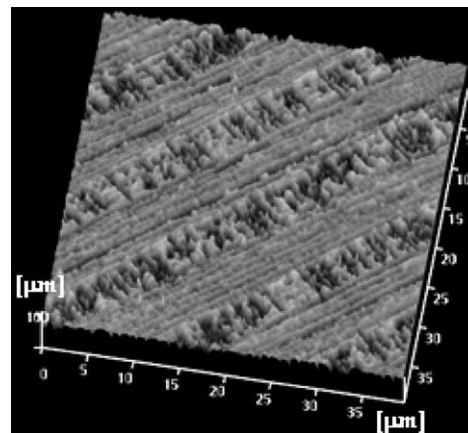


Fig. 7. Three-dimensional topographic image of the alternatively horizontal and vertical micro-groove pattern obtained by following the steps schematically shown in Fig. 2.

is entirely non-lithographic. The other contains $5\ \mu\text{m}$ wide stripes of alternating horizontal and vertical micro-grooves. Although the fabrication involves photolithography in supplement, the resolution involved in photolithography is low of $\sim 5\ \mu\text{m}$ only, and hence inexpensive microfabrication facilities would suffice.

Acknowledgements

We thank Prof B. Xu for useful discussions. This work is supported by the Research Grant Council of Hong Kong through the project HKUST6070/02P.

References

- [1] Kim E, Xia YN, Whitesides GM. *Nature* 1995;376:581.
- [2] Xia Y, Kim E, Zhao XM, Rogers JA, Prentiss M, Whitesides GM. *Science* 1996;273:347.
- [3] Kim YS, Suh KY, Lee HH. *Appl Phys Lett* 2001;79:2285.
- [4] Zhao XM, Xia Y, Whitesides GM. *Adv Mater* 1996;8:837.
- [5] Kim E, Xia Y, Zhao XM, Whitesides GM. *Adv Mater* 1997;9:651.
- [6] Wang Z, Zhang J, Xing R, Yuan J, Yan D, Han Y. *J Am Chem Soc* 2003;125:15278.
- [7] Cavallini M, Biscarini F. *Nano Lett* 2003;3:1269.
- [8] Kargupta K, Sharma A. *Phys Rev Lett* 2000;86:4536.
- [9] Kargupta K, Sharma A. *J Colloid Interface Sci* 2002;245:99.
- [10] Kargupta K, Sharma A. *Langmuir* 2002;18:1893.
- [11] Sehgal A, Ferreiro V, Douglas JF, Amis EJ, Karim A. *Langmuir* 2002;18:7041.
- [12] Higgins AM, Jones RAL. *Nature* 2000;404:476.
- [13] Lu N, Chen X, Molenda D, Naber A, Fuchs H, Talapin DV, et al. *Nano Lett* 2004;4:885.
- [14] Gleiche M, Chi LF, Fuchs H. *Nature* 2004;403:173.
- [15] Kevenhörster B, Kopitzke J, Seifert AM, Tsukruk V, Wendorff JH. *Adv Mater* 1999;11:246.
- [16] Karthaus O, Gråsjö L, Maruyama N, Shimomura M. *Chaos* 1999;9:308.
- [17] Du B, Xie F, Wang Y, Yang Z, Tsui OKC. *Langmuir* 2002;18:8510.
- [18] Lu G, Li W, Yao J, Zhang G, Yang B, Shen J. *Adv Mater* 2002;14:1049.

- [19] Kim YS, Lee HH. *Adv Mater* 2003;15:332.
- [20] Harkema S, Schaffer E, Morariu MD, Steiner U. *Langmuir* 2003;19: 9714.
- [21] Luo C, Xing R, Han Y. *Surf Sci* 2004;552:139.
- [22] Zhang HL, Bucknall DG, Dupuis A. *Nano Lett* 2004;4:1513.
- [23] Bruinink CM, Péter M, de Boer M, Kuipers L, Huskens J, Reinhoudt DN. *Adv Mater* 2004;16:1086.
- [24] Schäffer E, Thurn-Albrecht T, Russell TP, Steiner U. *Nature* 2000;403: 874.
- [25] Schäffer E, Harkema S, Roerdink M, Blossey R, Steiner U. *Adv Mater* 2003;15:514.
- [26] Tsang OC, Xie F, Tsui OKC, Yang Z, Zhang J, Shen D, et al. *J Polym Sci: Polym Phys* 2001;39:2906.
- [27] Rayleigh L. *Proc London Math Soc* 1878;10:4.
- [28] Brandrup J, Immergut EH, Grulke EA, editors. *Polymer handbook*. 4th ed. New York: Wiley; 1999.
- [29] Isaelachvili J. *Intermolecular surface forces*. 2nd ed. New York: Academic; 1992.
- [30] Tsui OKC, Wang YJ, Zhao H, Du B. *Eur Phys JE* 2003;12:417.
- [31] Zhang B, Lee FK, Tsui OKC, Sheng P. *Phys Rev Lett* 2003;91:215501.
- [32] Lee FK, Zhang B, Sheng P, Kwok HS. *Appl Phys Lett* 2004;85:5556.
- [33] Ibn-Elhaj M, Schadt M. *Nature* 2001;410:796.